Mottl, M.J., Davis, E.E., Fisher, A.T., and Slack, J.F. (Eds.), 1994
Proceedings of the Ocean Drilling Program, Scientific Results, Vol. 139

37. CORRELATION OF WELL LOGS, PHYSICAL PROPERTIES, AND SURFACE SEISMIC REFLECTION DATA, MIDDLE VALLEY, JUAN DE FUCA RIDGE[1]

Kristin M.M. Rohr[2] and Henrike Gröschel-Becker[3]

ABSTRACT

Synthetic seismograms calculated from well logs and shipboard physical properties measurements from Holes 858F and 857C have been correlated with surface seismic reflection records. Hole 858F was drilled in an active vent site and Hole 857C was drilled into nearby sediments with high heat flow. Physical properties measurements in unlogged portions of the holes were corrected for temperature, pressure, and anisotropy and merged with the log data; this allowed synthetic seismograms to be calculated from the seafloor to the bottoms of the holes. Log velocities in Hole 858F between 129 and 250 mbsf are 150–250 m/s higher than velocities in Hole 857C, which are in turn 200 m/s higher than those expected for abyssal turbidites. These increases occur despite probable velocity reductions associated with high in-situ temperatures. Site 858 was not logged for density, but physical properties measurements indicate that densities are as much as 0.5 g/cm^3 larger than normal abyssal turbidites. Site 857 has logged densities 0.2 g/cm^3 higher than normal abyssal turbidites, indicating that it too has been altered, but not as much as Site 858.

A strong increase in density and/or velocity occurs near the seafloor at Site 858; this increase occurs over a short distance relative to the wavelength of the seismic reflection data and reflects a large amplitude signal 30 ms beneath the seafloor. This event can be tentatively correlated to the change at 28 mbsf from lithologic Subunit IIA to IID which is more altered. Low core recovery and no logs from this interval render the exact configuration and nature of this transition unknown. The reflection has only been observed at Site 858 which indicates that the rapid increase in alteration with depth at Site 858 is a local phenomenon. At Hole 857C the transition from lithologic Subunit IIA to IIB is a gradual increase in degree of alteration that does not result in a strong reflection. At both sites the transition from sediments to interlayered basalt and sediments is marked by high-amplitude reflections. Modeling of the interlayered basalts and sediments at Hole 857D shows that these closely spaced, high-contrast layers result in an interference pattern when imaged by a low-frequency seismic source. Reflections are high in amplitude, but do not correlate to individual sill units.

INTRODUCTION

Ocean Drilling Program (ODP) Leg 139 drilled two sites in Middle Valley (Fig. 1) of the northern Juan de Fuca Ridge, in part, to compare a nearby sedimentary section (Site 857) with that associated with a hydrothermal vent (Site 858) 1.6 km away. Middle Valley, a rift valley formed by intermediate-rate spreading near the continental shelf, has received thick deposits of distal turbidites as nearby mountain belts were eroded during glacial periods (Davis and Villinger, 1992). Holes 857C and 858F were drilled through interlayered pelagic and hemipelagic sediments and turbidites into basalt and diabase. Velocity logs were run in both holes and at Hole 857C a density log was also run (Davis, Mottl, Fisher, et al., 1992). These data were combined with physical properties measurements collected from unlogged portions of the holes and then correlated to multichannel seismic reflection data.

This work is intended to provide ground truth for the reflection data, as well as insight into the large-scale velocity and density structure of sediments and igneous rocks at both sites. We had hoped that alteration of sediments would result in seismic reflections which could then be mapped in the rift valley. Gradual increases in alteration and stratigraphic heterogeneity, however, made this impossible.

METHODS

To correlate seismic reflection profiles with the log and physical properties data, we augmented log values with the physical properties data, computed synthetic seismograms, and compared the results to the seismic reflection data. Lithologic units based on core descriptions were then mapped onto the seismic reflection section. Descriptions of the definitions of lithologic units, measurements of physical properties, and running well logs can be found in Davis, Mottl, Fisher, et al. (1992).

Mean values of the processed long-spacing sonic logs were used for this analysis (Davis, Mottl, Fisher, et al., 1992). The data were converted from microseconds per foot (μs/ft) to microseconds per meter (μs/m) and zero values were deleted. The density profile was obtained with the lithodensity tool.

Sonic and density logs were integrated from depth into time based on the sonic log values for an output trace of 1-ms sample rate. Note that a depth sample over 1 m in material with a seismic velocity of 2000 ms^{-1} corresponds to a time interval of 1 ms on seismic reflection data. Thus, variations observed in the logs over the centimeter-scale are smoothed out at this stage. Reflectivity, or acoustic impedance, was computed using velocity and density values every millisecond (see Sheriff [1977] for a discussion of this standard procedure). This function was correlated with the outgoing pulse which we defined to be the reflection returned by the seafloor. The resulting synthetic was compared to the reflection data; changes were made to velocity and density logs until a good match was obtained. We chose to match reflectors with significant amplitudes and to ignore wiggles that were equivalent to noise level. Synthetic amplitudes are larger than measured amplitudes because these synthetics do not include multiples, attenuation, or transmission losses.

Logs were not run on the uppermost sections of the holes, so we constructed velocity and density profiles for the upper sedimentary section from shipboard physical properties values and added a water layer to generate seafloor reflections. The constructed logs extended from 0.0 to 129.0 m below seafloor (mbsf) in Hole 857C (Tables 1 and 2) and from 0.0 to 60.0 mbsf in Hole 858F; in the latter hole, densities obtained from shipboard measurements were used to the terminal depth of the velocity log because density logs were not available. Average density and velocity values assigned to depth intervals were compiled from whole-round core (GRAPE, *P*-wave logger) and discrete

[1] Mottl, M.J., Davis, E.E., Fisher, A.T., and Slack, J.F. (Eds.), 1994. *Proc. ODP, Sci. Results,* 139: College Station, TX (Ocean Drilling Program).

[2] P.O. Box 6000, Pacific Geoscience Centre, Geological Survey of Canada, Sidney, B.C. V8L 4R9, Canada.

[3] University of Miami, Rosenstiel School of Marine and Atmospheric Science, Marine Geophysics and Geology, 4600 Rickenbacker Causeway, Miami, FL 33149, U.S.A.

Table 1. Bulk densities used in unlogged section of Hole 857C.

Depth interval (mbsf)	Bulk density model (g/cm^3)	Comments
0.0–4.0	1.00 → 1.70	Seawater value at mudline; steep gradient reflecting thermal "consolidation" at shallow depths. Lithologic Unit I: fine-grained, hemipelagic sediment with minor fine-grained turbidites.
4.0–22.0	1.70	Constant density; presence of $CaCO_3$ bioclasts in upper section and then disseminated pyrite, biogenic Si in silty clays.
22.0–25.0	1.71	Small step representing increasing fine-grained sand fraction and thicker (>1 cm) turbidites as enter Unit IIA at 25.20 mbsf in Hole 857A (56.80 mbsf in Hole 857C).
25.0–80.0	1.72 → 1.80	Gentle gradient representing interbedded hemipelagic and turbiditic sediments that become more compacted with depth; first appearance of diagenetic $CaCO_3$, nodules; locally common pyrite as burrow linings and occasional nodules.
80.0–90.0	1.80 → 1.72	Moderately decreasing gradient observed in GRAPE data; due to decrease in turbidite frequency with corresponding increase in silt, clay (?). Poor recovery.
90.0–95.0	1.72	Lower density region is model best fit; moderately well indurated silty claystone predominant, although recovery poor.
95.0–110.0	1.72 → 1.86	Moderate gradient reflecting increasing frequency of silty fine sandstone turbidites (Hole 857A) and carbonate nodules recovered from 95.20 to 114.50 mbsf in Hole 857C. Selective carbonate cementation observed to increase with depth.
110.0–115.0	1.86	Constant density; carbonate nodule-rich siltstone lithology inferred. Top of Unit IIB is at 114.43 mbsf in Hole 857C (101.50 mbsf in Hole 857A) and differentiated from Unit IIA by its moderately to well indurated character.
115.0–120.0	1.86 → 2.06 → 1.86	Density maximum due to carbonate nodule concentration in fine sandstone modeled as a truncated spike; $CaCO_3$ cementation in claystone also common.
120.0–129.0	1.86	Constant density region reflecting claystone calcite cement and decreased fine-grained sandstone content. Model ties into log at 129.0 mbsf.

sample (penta-pycnometer, balance, digital sound and Hamilton frame velocimeters) data from logged boreholes and from nearby Holes 857A and 857B (Shipboard Scientific Party, 1992a) and Holes 858B, 858C, 858D, and 858F (Shipboard Scientific Party, 1992b).

Because lab and log measurements occurred at different pressures and temperatures, we tried to correct lab measurements of density and velocity back to values more representative of in-situ conditions. Higher than normal temperatures of the upper crust in Middle Valley were of particular concern. The effect of increasing pressure on densities of most rocks and minerals is small unless porosity is modified (Johnson and Olhoeft, 1984), as occurs when cracks in hard rock close with depth. Density changes in response to increasing temperature are generally small (Skinner, 1966) and the lack of experimental data for sediments or their mineral constituents prevented any type of semi-quantitative analysis of this effect. We therefore assumed that the shallow sediments included in the model had higher densities than normal owing to alteration from the high-temperature regimes described at both sites and did not make pressure or temperature corrections to laboratory density data (Table 1).

Several calculations and corrections were made to shipboard sediment velocity data prior to incorporation into the models. A general agreement between vertical shipboard compressional-wave velocities (parallel to core axes) and sonic log velocities (Shipboard Scientific Party, 1992a) suggested that little correction was needed to achieve a "match" between unlogged and logged sections of the holes. An attempt to correct velocities for rebound resulted in a significant mismatch between the log and lab data so was rejected. We corrected the sediment velocity data for pressure by using the method outlined in Hyndman and Drury (1976). An evaluation of the effects of larger-scale drilling-induced fracture porosity on borehole velocity data is complicated by the poor-quality sonic data and is beyond the scope of this paper.

To construct velocity values for the unlogged interval we first assembled a suite of vertical compressional-wave velocities (V_v). These values were collected with the digital sound velocimeter on split-cores and were calculated from the Hamilton frame data measured in the horizontal direction (V_h). Velocity anisotropy was observed in oriented cubes cut from lithified sediment below 153.49 mbsf at Hole 857C (Table 3), but was not measured above this depth because cubes could not be cut. Twin-blade measurements were made in two directions. An anisotropy factor that varied with depth was applied to V_h data to obtain V_v (Table 4). A linear best-fit curve was calculated for anisotropy data from 153.49 to 240.93 mbsf and forced through a value of zero at the seafloor (Fig. 2); deeper data, which showed a shift to an average of 18.9%, were excluded (Table 3).

Next, we applied a temperature correction. Experimental data show that velocities generally decrease with increasing temperatures for both saturated and dry consolidated sedimentary rocks. This change can be up to 10% for a temperature range of 20° to 200°C (Shumway, 1958; Timur, 1977, and references therein). The formation of new cracks with varying aspect ratios as a result of differential thermal expansion of constituent minerals may cause additional decreases in

Table 2. Velocities used in unlogged section of Hole 857C.

Depth interval (mbsf)	Corrected velocity model (m/s)	Comments
0.0–25.0	1500 → 1495	Seawater value above mudline; low values for soft sediment in Unit I below mudline to 19.60 mbsf (Hole 857A). Low-velocity interval required to match seafloor reflector amplitude.
25.0–40.0	1534	Step increase as enter Unit IIA at 25.30 mbsf in Hole 857A; fine-grained sandstone fraction increases in thicker (>1 cm) turbidites (Hole 857A).
40.0–45.0	1563	Small step increase is model best fit.
45.0–60.0	1580	Step increase reflects appearance of diagenetic $CaCO_3$ and some nodules in firm silty clays (Hole 857A).
60.0–70.0	1604	Step increase represents increasing cementation of stacked fining-upward turbidite sequences and locally common pyritized burrows.
70.0–85.0	1589	As above with more calcite, carbonate, pyrite nodules and lithification.
85.0–90.0	1589 → 1495	Gently decreasing gradient consistent with limited PWL and DSV/HFV data; perhaps due to local decrease in coarser grained material (?). Poor recovery (Hole 857A).
90.0–115.0	1495 → 1742	Moderately increasing gradient reflects increasingly indurated material as Unit IIB is encountered at 101.50 mbsf in Hole 857A (114.50 mbsf in Hole 857C); more carbonate cement in silty clays, thicker silty fine sandstone turbidites, pyrite with depth (Hole 857A) and carbonate nodules in siltstone (Hole 857C).
115.0–120.0	1742 → 2000 → 1745	Zone of carbonate nodules recovered at Hole 857C is modeled as a broad, flat-topped spike; 2000 m/s peak gives best match to reflector.
120.0–129.0	1750	Constant velocity region reflecting calcite cement in claystone (Hole 857C) that is moderately to well indurated. Model ties into sonic log at 129.0 mbsf.

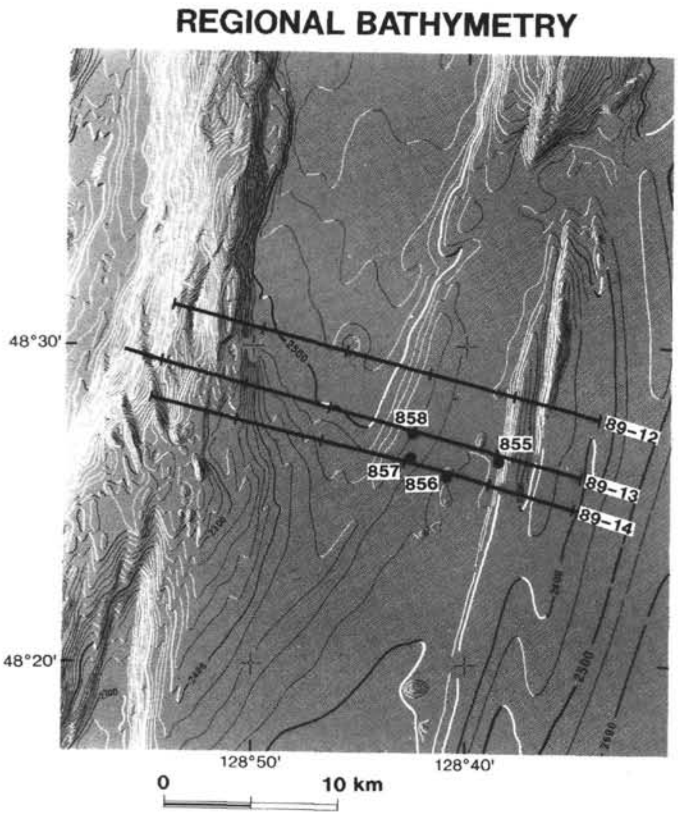

Figure 1. Location of Leg 139 sites and multichannel seismic reflection data in Middle Valley, Juan de Fuca Ridge. Bathymetry in meters.

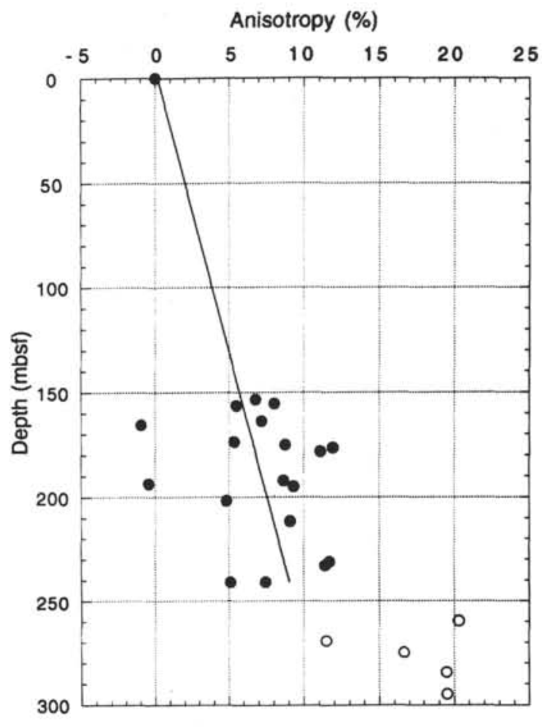

Figure 2. Anisotropy values from Hole 857C as measured on lithified cubes. The linear fit was forced through zero at the seafloor. Only values above 250 mbsf (filled circles) were included in the fit.

Table 3. Anisotropy of velocity measurements in Hole 857C (after Scientific Shipboard Party, 1992a, table 37 and fig. 75B).

Core, section, interval (cm)	Depth (mbsf)	Vertical *P*-wave velocity (m/s)	Horizontal *P*-wave velocity (m/s)	Anisotropy (%)	Comments
139-857C-					
13R-1, 39–41	153.49	1776	1901	6.80	Silty claystone and clayey siltstone.
13R-2, 89–91	155.49	1692	1834	8.05	As above.
13R-3, 29–31	156.39	1876	1982	5.50	As above.
14R-1, 98–100	163.78	1752	1883	7.21	Massive silt and silty clay.
14R-2, 128–130	165.56	2107	2087	–0.95	Massive to convolute-bedded sandy silt at base of turbidite.
15R-1, 110–112	173.70	1779	1877	5.36	Massive silty clay and minor silty sand
15R-2, 120–122	175.20	1743	1903	8.78	As above.
15R-3, 107–109	176.54	1762	1985	11.9	Massive silty clay that is locally moderately bioturbated
15R-4, 118–120	178.24	1844	2060	11.07	As above.
17R-1, 34–36	192.24	1777	1938	8.67	Silty clay at top of turbidite sequence.
17R-2, 45–47	193.85	2110	2101	–0.43	Fine- to medium-grained basal turbidite sand and silt with sedimentary structures.
17R-3, 7–9	194.97	1836	2016	9.34	Silty clay in upper turbidite sequence.
18R-1, 23–25	201.83	2118	2223	4.84	Semi-lithified silty clay interbedded with siltstone and fine sand.
19R-1, 41–43	211.71	1921	2104	9.09	Silty clay in upper turbidite sequence.
21R-1, 50–52	231.10	1924	2163	11.7	Silty claystone with well-preserved parallel laminae.
21R-2, 81–83	232.91	1977	2216	11.4	As above.
22R-1, 55–57	240.85	2036	2194	7.47	Interbedded indurated silty claystone and parallel-layered siltstone.
22R-1, 93–95	240.93	2284	2404	5.12	As above.
24R-1, 42–44	259.62	1908	2339	20.3	Moderately indurated silty clay interbedded with siltstone; parallel laminated.

Table 4. Anisotropy and temperature corrections for velocity measurements in Hole 857C.

Depth interval (mbsf)	*P*-wave velocity[a] (m/s)	Anisotropy factor[b] (%)	Calculated V_v (m/s)	Borehole T/ T-23 (°C)	T correction (m/s)	Corrected V_v (m/s)
0.0–1.0	1500 → 1480	0.00		1.7/–21.3	+14.4	1494
1.0–20.0	1520 (v)	0.35		14.2/–8.8	+6.0	1526
20.0–25.0	1533 (v)	0.80		17.8/–5.2	+3.6	1537
25.0–38.0	1539 (v)	1.00		30.1/7.1	–4.9	1534
38.0–44.0	1569 (v)	1.50		31.2/8.2	–5.7	1563
44.0–60.0	1594 (v)	1.75		42.6/19.6	–13.6	1580
60.0–70.0	1623 (v)	2.25		49.7/26.7	–18.6	1604
70.0–86.0	1657 (h)	2.45	1616	61.1/38.1	–26.7	1589
86.0–92.0	1616 → 1575 (h)	3.15	1525	65.3/42.3	–29.7	1589 → 1495
92.0–115.0	1525 → 1847 (h)	3.40	1784	81.7/58.7	–42.0	1495 → 1742
115.0–120.0	1784 → 2038 (h) → 1851 (h)	4.20	1952 → 1773	85.2/62.2	–44.7	1742 → 1907 → 1728
120.0–129.0	1795	4.35	1717	91.6/68.6	–49.5	1668

[a] Direction given in parentheses if discrete sample (v = vertical; h = horizontal).
[b] $V_h > V_v$

velocity (Toksöz et al., 1976) in addition to those resulting from changes in the moduli of the solid and fluid components (Timur, 1977).

Sediment temperatures were estimated from the least-squares linear gradient of 0.71°C/m from the two reliable water sampler temperature probe data in Hole 857C (fig. 97A and table 45; Shipboard Scientific Party, 1992a). Temperature profiles are presented in this volume by Davis and Wang but we do not feel that application of these new values will significantly change the results presented here. Seismic reflections result from rapid changes in physical properties; changing the value of a linear gradient applied to the entire section will not effect the correlation of log values to seismic reflection data. Temperature effects were difficult to correct for. Values used in the velocity corrections probably represent the maximum temperature for these intervals. The temperature difference between the inferred in-situ temperatures and the average shipboard laboratory temperature of 23°C was multiplied by a pressure-dependent factor relating change in velocity to change in temperature. As no data for clay or hemipelagic mud were available in the literature, this factor was developed from the data of Timur (1977) for Berea and Boise sandstones, for which the change in velocity with increasing temperature was approximately linear to 200°C. The correction curve utilized a velocity-temperature relation of $-8.5 \cdot 10^{-4}$ km/s °C calculated from the Boise sandstone data at 34.5

MPa and $-5.0 \cdot 10^{-4}$ km/s °C at 14.0 MPa, based on the relation calculated for the Berea sandstone between 7.8 and 19.5 MPa. The latter relation was multiplied by 2 to account for porosity differences between the two samples. Results are given as corrected V_v in Table 4 and compared to uncorrected values in Figure 3.

A weakness in applying this correction is that the sediments at Sites 857 and 858 contain significant amounts of clay and silt (e.g., Table 2) (Shipboard Scientific Party, 1992a); the correction is probably more appropriate at greater depths where turbidites contain more sand. The resulting temperature-correction to velocity at 129.0 mbsf, for an estimated temperature of 92°C is –3%. This amounts to 50 m/s and may be small considering other uncertainties such as downsection variations in lithology, porosity, and density. These are especially difficult to quantify because recovery was less than 10%.

Integrating physical properties data with the log values involved a certain amount of trial and error because physical properties measurements are taken at discrete locations whereas the seismic waves respond to an integrated suite of values over much greater distances. For example, the seismic wavelength of 30 Hz energy in material with a velocity of 1800 m/s is 60 m. The major decision made when constructing a log profile was whether to connect the physical properties values with a gradient or discrete steps. The latter tends to produce reflections whereas the former does not. Core descriptions were also used to make this decision, but the ultimate discriminant was whether the synthetic matched the reflection data or not.

The seismic reflection data collected in 1989 (Rohr et al., 1992) were recorded on 144 channels, but for correlation we used only the trace nearest to the airgun array from each common midpoint gather. The stacked traces are averages of amplitudes across 3.6 km of offset and we wanted to match only the normal-incidence amplitudes. Reflections from the sill sequence varied strongly in their amplitudes from 260 to 3860 m offset.

When correlating seismic reflection data with measurements made in a drill hole, it is worth remembering the vastly different scales of measurement. Although we frequently refer to shotpoints as individual points on the Earth's surface, sound waves, in fact, spread spherically and are reflected back from a region of the subsurface. The first Fresnel zone is the main contributor to the pulse detected by the streamer; for a 30-Hz source in 2200 m of water the first Fresnel zone is 500 m in diameter. This "footprint" of the seismic source is equivalent to the area covered by the hydrothermal vents drilled in Site 858 (Fig. 4). Thus, the seismic reflection data represent an average of the physical properties measured over an area, whereas drilling brings up a 6.6-cm-diameter core that may or may not be similar to that average. Log values in turn are measured in the hole on the scale of meters; they are considered more representative of in-situ properties, but again, may not represent the large area sampled by the seismic waves.

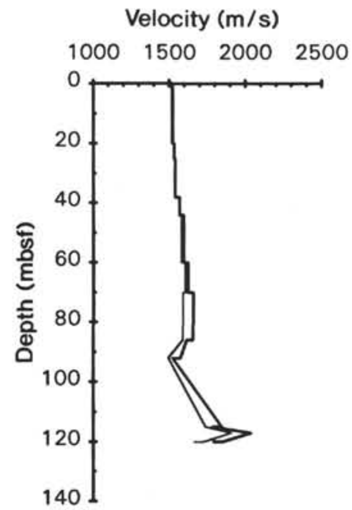

Figure 3. Profile of velocity constructed from lab measurements of velocity (Table 4). Heavy line is V_v; lighter line is velocity corrected for anisotropy and temperature.

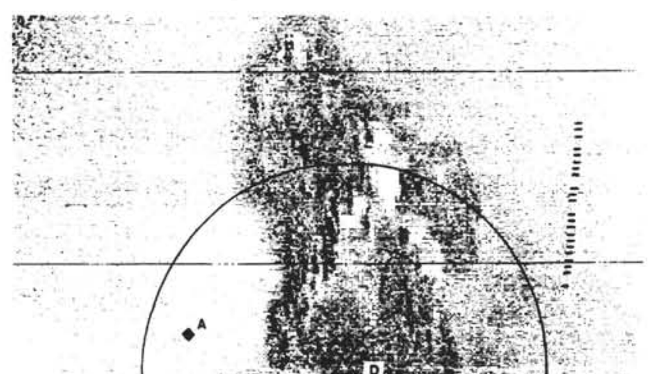

Figure 4. First Fresnel zone for 30-Hz energy plotted on sidescan image of the hydrothermal vent sampled by Hole 858. This region is the primary contributor to the pulse detected by the streamer and interpreted as the seafloor reflection (after fig. 9, Shipboard Scientific Party, 1992b). Letters refer to Holes 857A–857D and Holes 857F and 857G.

DATA ANALYSIS AND RESULTS

Correlation of Site 857

The main events in the seismic reflection data over Hole 857C are the seafloor at 3.29 s and an equally strong reflection at 3.77 s (Fig. 5). Smaller amplitude reflections occur between them. Hole 857C occurs between two normal faults which have small offsets down to the west (Rohr and Schmidt, this volume). The lithodensity tool measured bulk densities between 101 and 513 mbsf and the sonic tool measured transit times between 129 and 500 mbsf. A synthetic seismogram was computed from the logs between 129 and 513 mbsf without adding shallower data. This seismogram included a series of events from 129 to 200 m and a strong reflection from the basalt layer. We correlated the first events to reflections seen at 3.46 s and the basalt to the reflection at 3.77 s. The time interval between the events at 3.46 and 3.77 s on the synthetic seismogram is a good match to the time between events observed on the seismic reflection data. A moderately strong event was recorded on the seismic reflection data at 3.68 s, but there is no indication from the logs of significant changes in velocity or density. This discrepancy is probably the result of the larger footprint of the reflection data as compared to the drill hole.

The top 129 m of log was constructed first by connecting corrected physical properties measurements (Tables 1 and 2) with gradients (Fig. 6). At the seafloor the seismic velocity does not change significantly, but density increases from 1.0 to 1.7 g/cm^3. In the top 80 mbsf neither

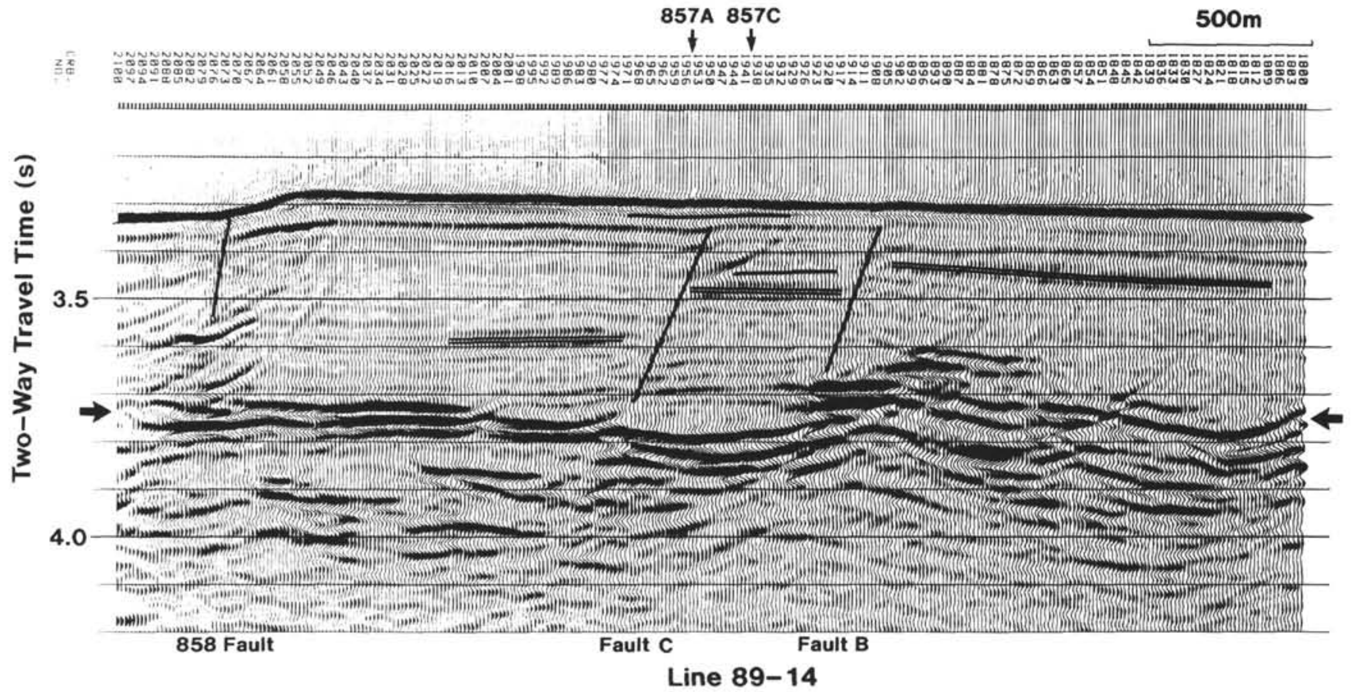

Figure 5. Migrated multichannel seismic reflection line 89-14 over Site 857 (after Rohr and Schmidt, this volume). The seafloor is at 3.3 s; arrows indicate bright reflections that have been interpreted as sills. The "858 fault" is a major-offset fault that runs the length of Middle Valley. Faults "B" and "C" are two small-offset normal faults. Double lines mark a reflector that can be correlated across the faults.

property changes much, which is not surprising considering that these sediments were described as unconsolidated to "weakly indurated" (Shipboard Scientific Party, 1992a). Small events observed in the top 200 ms of reflection data could not be reproduced given the interval at which physical properties measurements were made. Both density and velocity curves have a local minimum at 87.7 mbsf. This corresponds to a silty claystone that is otherwise undistinguishable from neighboring cores. The positive velocity gradient below 87.7 mbsf is probably caused by the appearance and gradual increase of carbonate cement and carbonate nodules, which first occur near 100 mbsf. High velocities of 2012, 1699, and 2372 m/s were measured between 114.59 and 114.88 mbsf in silty claystone (Shipboard Scientific Party, 1992a). We ran a model with a high-velocity layer at this depth, but did not find a corresponding reflection in the seismic data. If this layer is surrounded by velocity gradients or is not a regionally significant feature, it would not reflect seismic energy. Our final model does not include this layer. In the synthetic the time interval between the seafloor and the event which was correlated above to a reflector at 3.46 s was smaller than that observed on the reflection data. Velocities in the top 129 m of the log were accordingly reduced by 13% to match the time interval between the seafloor and the reflector at 3.46 s.

At Hole 857D a layered basalt-sediment sequence was drilled from 471 mbsf to 936 mbsf. Gamma ray and resistivity logs from this interval clearly identify the interlayered sediment and basalt sills (Shipboard Scientific Party, 1992a). To see what the seismic response of these layers was, we digitized their thicknesses and assigned values of 394 µs/m (2538 m/s) and 2.3 g/cm^3 to the sediment and 213 µs/m (4695 m/s) and 2.8 g/cm^3 to the basalt based on logged values observed in basalt and interlayered sediments at the base of Hole 857C. The sequence was then attached to the end of logs from Hole 857C (Fig. 7). The resulting synthetic traces are clearly the sum of an interference pattern generated by reflections from the tops and bottoms of closely spaced sills. The synthetic traces do not match the sequence of peaks and troughs in the seismic data. The general pattern is similar, but the problem is too non-unique to attempt a "perfect" fit.

As a last step, lithologic units (Shipboard Scientific Party, 1992a) were correlated to the seismic reflection section (Fig. 8). Lithologic units were defined from core descriptions; only the transition from Subunit IIB to IIC was logged. Unit I, Holocene to upper Pleistocene sediments, occurs from 0 to 25 mbsf in Hole 857A. A small down-to-the-east normal fault (Rohr and Schmidt, this volume) occurs between Holes 857A and 857C and Hole 857C was not cored between 4 and 36 mbsf. Thus, we can not identify the Unit I/II boundary in Hole 857C. Little change occurs in velocity or density measured on lab samples in Hole 857A between 0 and 40 mbsf (near the Unit I/II boundary) so we would expect only a small-amplitude event, if any, at this boundary. The contact between Subunits IIA and IIB was defined at 114.5 mbsf and marks a gradational increase in induration. It falls 150 ms bsf within a region of small-amplitude reflections at 3.43 s. The top of Subunit IIC is easily identified in the reflection data.

Correlation of Site 858

The Site 858 seafloor reflection at 3.285 s has a large amplitude and is closely followed (30 ms bsf) by a second reflection. A moderately large reflection occurs at 3.41 s and a large reflection at 3.57 s (Fig. 9). The seafloor reflections are of unusually high amplitude around the vent (Rohr et al., 1993) and the event 30 ms under the seafloor has only been observed under the hydrothermal vent. The sonic log collected data from 57 to 273 mbsf in Hole 858F (Shipboard Scientific Party, 1992b). The top of the log was noisy, but the log appears to give more consistent values below 100 mbsf (Fig. 10).

The first synthetic was computed using the sonic log and a default density of 1 g/cm^3. It produced reflections that could be correlated to reflections at 3.41 s (140 ms bsf) and 3.57 s (300 ms bsf). An interval at 110 mbsf on the log is about 1000 m/s higher in velocity than surrounding layers. At first glance these measurements appear to be noise, but this layer, in fact, produces a reflection which can be correlated with an event at 3.41 s in the seismic section. This reflection is nearly twice as large as other sedimentary reflectors. We cannot be sure what kind of rocks reflected the seismic energy, because this interval yielded only 5% recovery consisting of unremarkable sediments (Shipboard Scientific Party, 1992b) and no physical properties were measured in this interval. The interval time computed from the

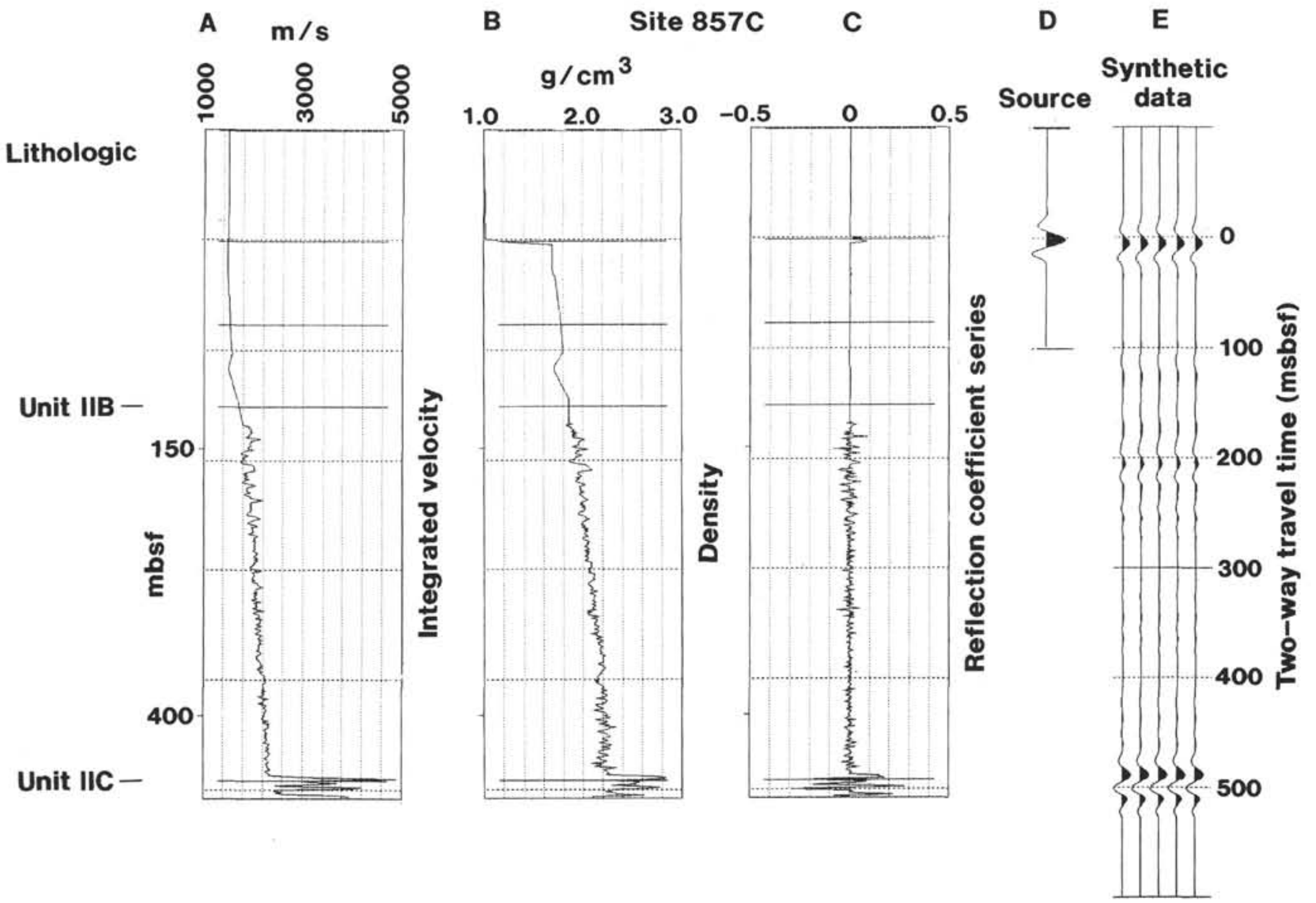

Figure 6. Calculation of synthetic seismograms. **A.** Velocity log. **B.** Density log. **C.** Reflectivity sequence. **D.** Source function. **E.** Synthetic traces. Source was taken from seafloor reflection of multichannel data.

synthetic between this reflector and basalt was too short compared to the reflection data, so velocities in this interval were reduced by 10% for a better match.

The problem remains to try and model the seafloor reflection and the reflection immediately following. Only 2% of the section was recovered, but other lines of evidence exist to infer what the top, unlogged 57 mbsf are like. Rocks in this section range from hemipelagic and turbidite sediments to "silicified and hydrothermally altered, interbedded, hemipelagic and turbiditic strata" (Shipboard Scientific Party, 1992b). On the basis of drilling rate, an indurated cap is thought to exist at 30 mbsf. Physical properties measurements at Hole 858F between 46 and 66 mbsf yielded velocities of 2673 to 3942 m/s and densities of 2.25 to 2.46 g/cm^3 which are considerably higher than usually encountered at similar depths in abyssal turbidites. Seafloor around the vent has a reflection coefficient of 0.6–0.7 (Rohr et al., in press), twice as high as reflection coefficients expected from abyssal turbidites. The wavelength of the seismic energy in water is 50 m so the reflection's amplitude depends on velocity and density within the top 50 m of the sediments. Yet coring by Goodfellow et al. (in press) penetrated up to 3 m of unconsolidated sediments. The reflection 30 ms bsf could be from the top of the indurated cap. For interval velocities of 1500–2000 m/s between this event and the seafloor, the reflector would occur at depths of 22.5 to 30 mbsf. The computed interval velocity between the reflection at 3.41 s and the seafloor is 1760 ± 60 m/s. This indicates that velocities greater than 2000 m/s (obtained from physical properties measurements) do not exist throughout the top 110 mbsf; lower velocity material is either intercalated with, or underlies high velocity material.

Forward modeling of synthetic seismograms is notoriously nonunique, but given the constraints just outlined we present below one possible solution to match results from Leg 139 with the seismic reflection data.

Matching the amplitude of the seafloor reflection required inserting a high-velocity spike (Fig. 10). This is because these synthetics treat seismic energy as rays, not waves. In reality the wave is responding to velocity and density in the top 50 m of sediments, but this standard normal incidence routine computes reflection coefficients from physical properties every meter. Synthetics that compute the wave response (e.g., reflectivity algorithm) are typically invalid at normal incidence. To be consistent with coring data we modeled varying thicknesses of soft sediment over a hard layer and found that up to 5 m of unconsolidated sediment was undetectable with a 30-Hz wavelet. We conclude that the increase in alteration with depth noted by Goodfellow et al. (in press) results in altered, hard material several meters below the seafloor. While the value of velocity used is arbitrary, high velocity or density layers must exist to produce such a reflection. However, we must also remain consistent with a computed interval velocity of 1760 m/s.

Physical properties measurements were used to fill in the top of the velocity log and adjusted to fit the observed reflection traveltimes (Fig. 10). We treated the velocity measurements in the top 20 m as isovelocity layers; in other words, a lab measurement is considered to be representative of the section until the next measurement is encountered. To make a smooth transition from the physical properties measurements into the log data we treated the high-velocity values at 46 and 55 mbsf as spikes, because treating them as a single high-velocity

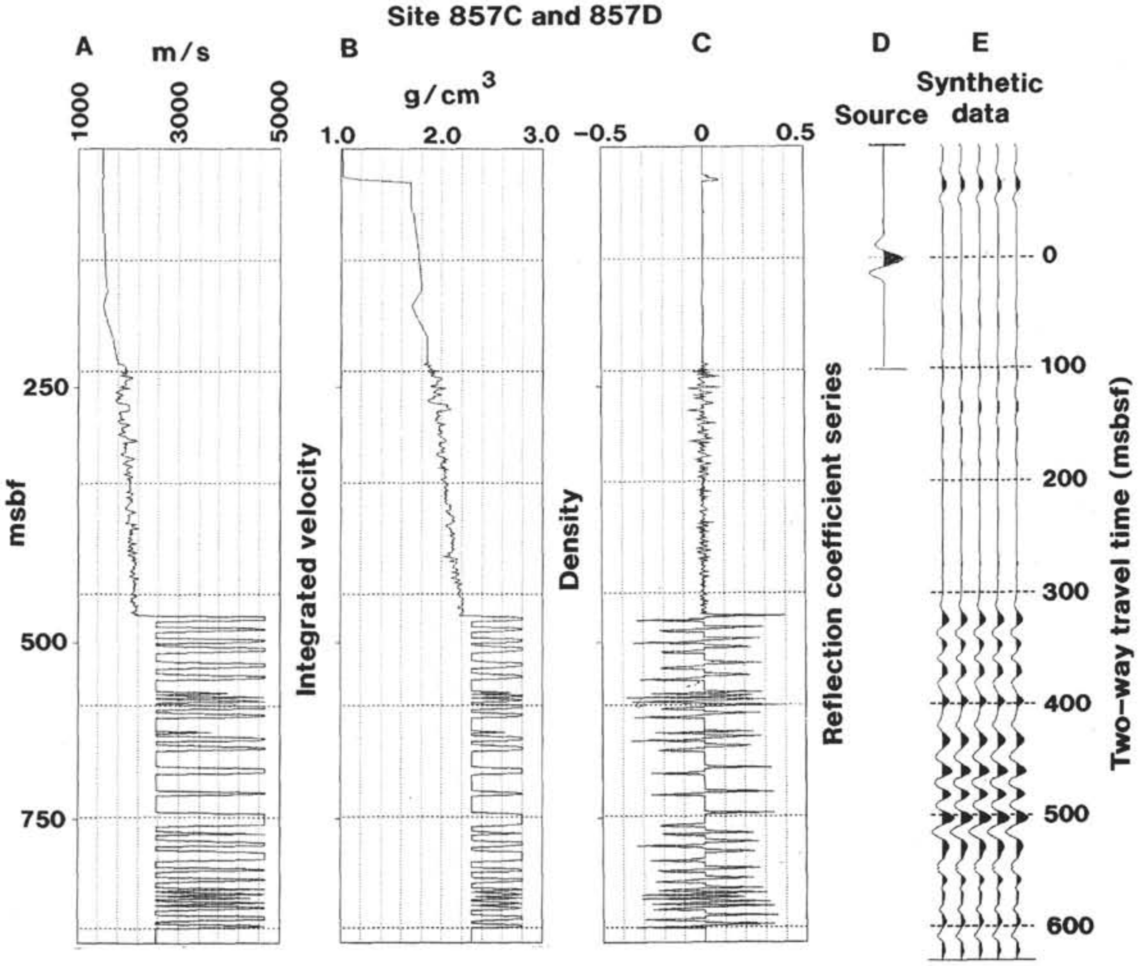

Figure 7. Calculation of synthetic seismograms. **A.** Velocity log. **B.** Density log. **C.** Reflectivity sequence. **D.** Source function. **E.** Synthetic traces. Source was taken from seafloor reflection of multichannel data.

layer resulted in synthetic reflections which were not observed in the data. Physical properties velocity data are significantly greater than the original log between 40 and 100 mbsf. We believe that the log data are more representative of in-situ conditions and constructed a smooth function between 40 mbsf and the top of the log values.

No density log was run at Site 858 so we constructed a profile based on the laboratory measurements of bulk density at Holes 858B (0.7 mbsf), 858D (1–7 mbsf), 858C (13–37 mbsf) and 858F (47–250 mbsf) (Fig. 10). In the top 37 m sample spacing is 1–5 m; between 37 and 100 mbsf samples are spaced every 10 m and below this samples are spaced every 50 m. Since the holes were drilled within the first Fresnel zone of the seismic reflection data (Fig. 4), combining data from different holes is legitimate. We connected the deeper, more sparse measurements with gradients to avoid spurious reflections in the synthetic seismogram. By analogy to the velocity log, we connected density values between 40 and 94 mbsf with linear gradients. At the first occurrence of basalt we modeled a step function in density.

Lithologic units at Hole 858F consist of Subunit IIA (0–28 mbsf), Pleistocene interbedded hemipelagic and turbiditic sediments and Subunit IID (28–250 mbsf), which consists of similar sediments with breccia, carbonate, and anhydrite and local zones rich in sulfides (Shipboard Scientific Party, 1992b). As modeled, the top of Subunit IID is coincident with the reflection below the seafloor (Fig. 11). The strong reflection at 3.57 s correlates to the first basaltic layer, the top of Unit V.

DISCUSSION

Logged velocities of each hole can be compared between 130 and 260 mbsf, the interval of overlapping measurements. The maximum values of Hole 857C and minimum values of Hole 858F overlap, but a linear fit to each function shows that velocities in Hole 858F start out approximately 150 m/s higher and have a higher gradient than in Hole 857C. The velocity gradient over this interval is 2300 ms^{-1}/m in Hole 858F and 1400 ms^{-1}/m in Hole 857C.

Both velocity and density, as measured by logging in Holes 857C and 858F, are higher than expected for terrigenous sediments (i.e., distal turbidites) (Fig. 12) at equivalent depths. Hamilton (1976, 1980) has published several papers summarizing his and others' results of physical properties measurements on deep-sea sediments; values for terrigenous sediments were obtained by averaging measurements at 20 different sites. No error bars are available for these averages. The velocity-depth function at Hole 857C is 200–250 m/s higher than for normal terrigenous sediments between 130 and 250 mbsf and at Hole 858F it is 300–500 m/s higher. In this interval the velocity gradient for turbidites is 1 ms^{-1}/m; at Hole 857C it is 1.4 and at Hole 858F it is 2.3. The density log from Hole 857C is up to 0.2 g/cm^3 higher than expected and has a similar gradient as the curve for terrigenous sediments (Fig. 13).

Interval velocities calculated using Dix equations (Dix, 1955) on a common-midpoint gather (cmp) centered at Hole 857C are close to

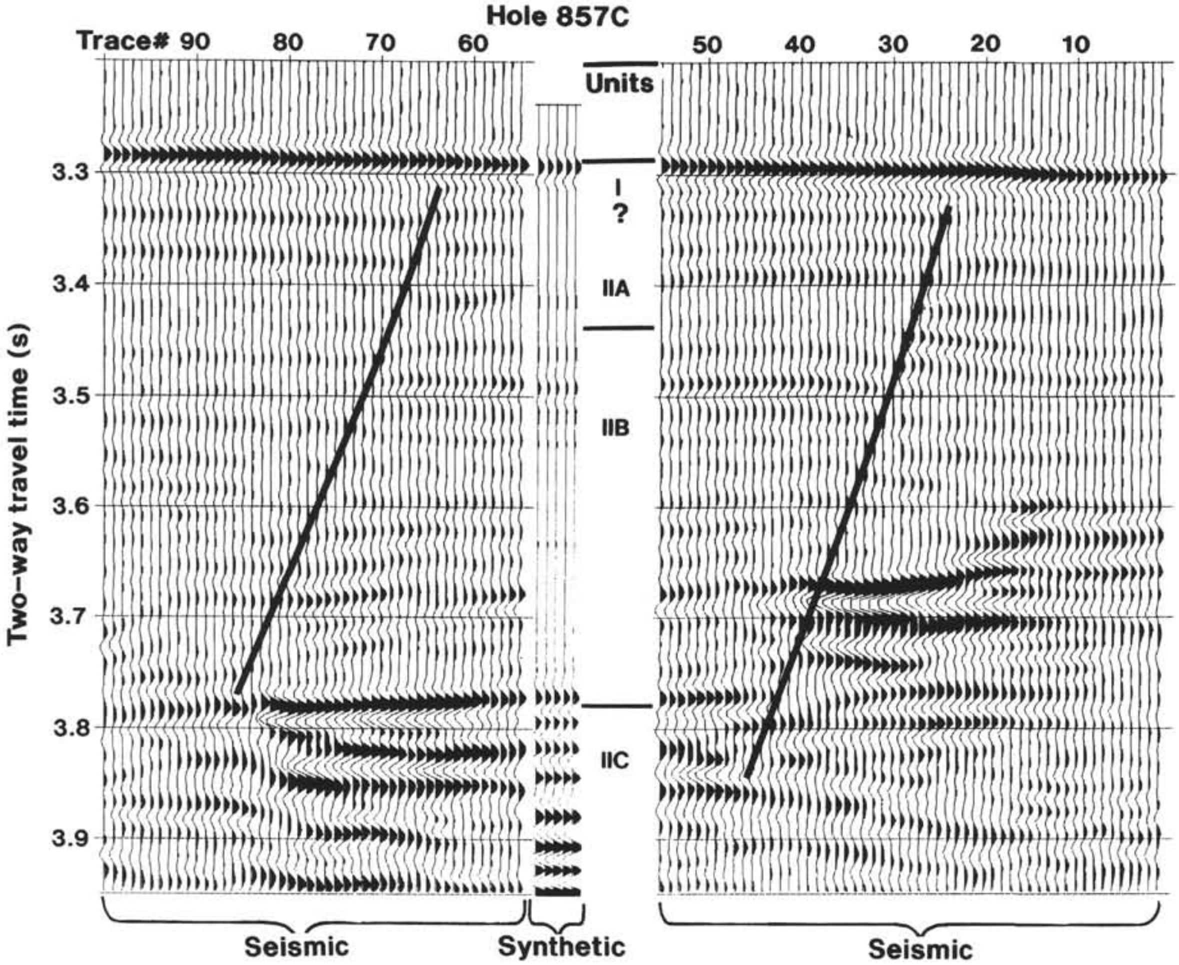

Figure 8. Synthetic seismograms compared to near traces around the drill hole. The seafloor and basalt are the strongest reflectors; a sequence of sedimentary reflectors at 3.46 ms can also be matched. The transition from lithologic Subunit IIA to IIB is subtle and impossible to correlate across the faults.

logged values, but are higher at Hole 858F (Fig. 14, Table 5). At Hole 857C the Dix interpretation was only reliable for the first 320 ms because of lateral heterogeneity of the basalt reflector within the cmp. Nearby gathers were also unreliable because of nonhyperbolic behavior of the basalt reflections. The interval velocity is 1716 m/s between 3.26 and 3.46 s (Unit I and Subunit IIA) and 1873 m/s between 3.46 and 3.58 (within Subunit IIB). At Hole 858F the Dix solution gave 1962 m/s for the top 108 m and 2550 m/s between 108 and 130 mbsf. Both values are hundreds of meters per second higher than the logged values. Velocity heterogeneity or seismic anisotropy at Site 858 could account for the discrepancy. Because the lab samples were up to 20% faster in the horizontal direction than the vertical, wide-angle reflections should travel faster through the section than normal incidence energy. An analysis of possible effects of anisotropy on the wide-angle data, however, suggests that lateral heterogeneity may be the more important effect (J. Dellinger, pers. comm., 1993).

Table 5. Interval velocities calculated from log-to-seismic correlation and Dix technique.

Hole	Dix interval velocity (m/s)	Depth interval (mbsf)
857C	1716	0–172
	1873	172–285
858F	1962	0–108
	2550	108–130

CONCLUSIONS

At both sites the most prominent reflectors are the seafloor and basalt flows and sills. Modeling of the basalt section at Hole 857D shows that a sequence of 29 basalt layers in a 480-m-long section can result in an interference pattern consisting of only eight cycles when the source is dominantly 30 Hz. At Site 858 another strong event occurs 30 ms below the seafloor reflection that is not observed on any other multichannel line. It can tentatively be correlated with the top of Subunit IID, the silicified and hydrothermally altered sediments which comprise the rest of the hole. It must be stressed that the low recovery in this interval and lack of logging data severely limit a lithologic interpretation of the strong impedance contrast detected by the seismic data. In addition at Hole 858F a layer at 110 mbsf with velocities 1000 m/s higher than surrounding layers can be correlated with a reflection at 3.41 s. In Hole 857C the Unit I to Unit II boundary was not cored and the transition from Subunit IIA to IIB is a gradual increase in alteration. It can be correlated to a group of small-amplitude reflections.

Velocities between 129 and 250 mbsf are 150–250 m/s higher in Hole 858F than in Hole 857C and velocities in both holes are higher than expected for abyssal turbidites. Hole 857C is 0.2 g/cm^3 higher in density between 129 and 450 mbsf than expected for abyssal tur-

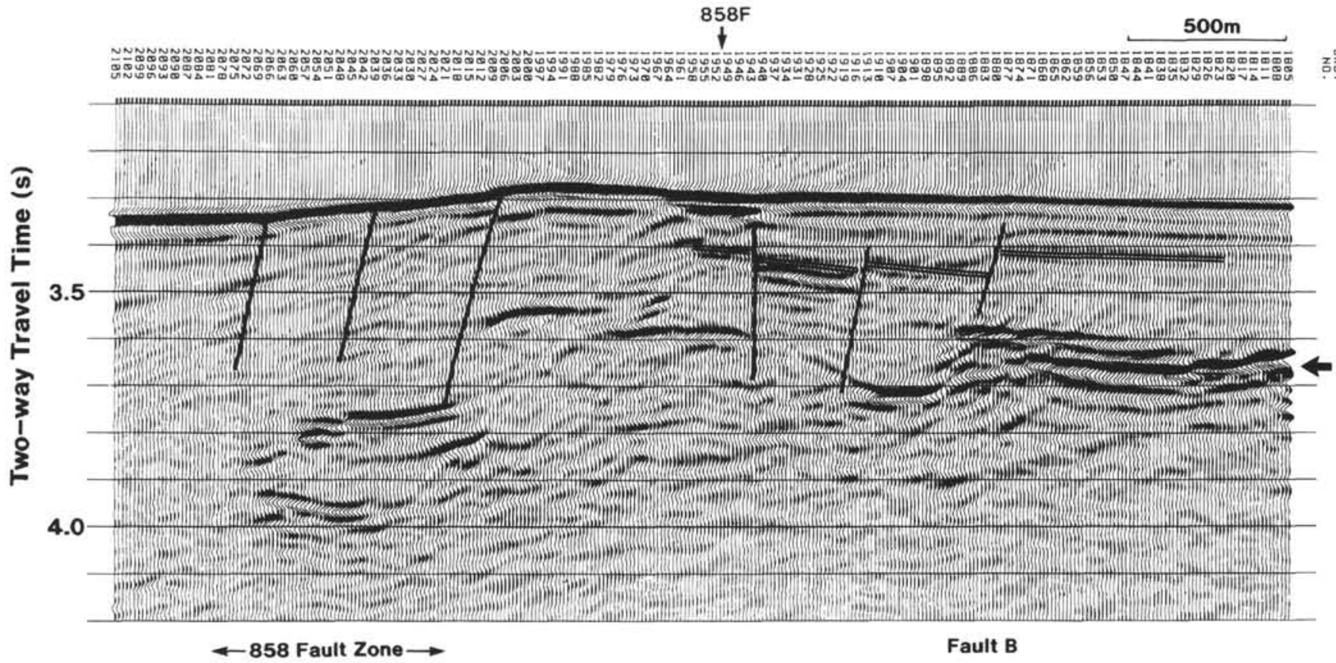

Figure 9. Section of migrated multichannel seismic reflection line 89-13 over Site 858 (from Rohr and Schmidt, this volume). Note bright reflector immediately below seafloor reflection. This profile is only 1.6 km north of Figure 5, but has a very different set of basalt reflections. Arrow at right indicates top of sill-sediment sequence.

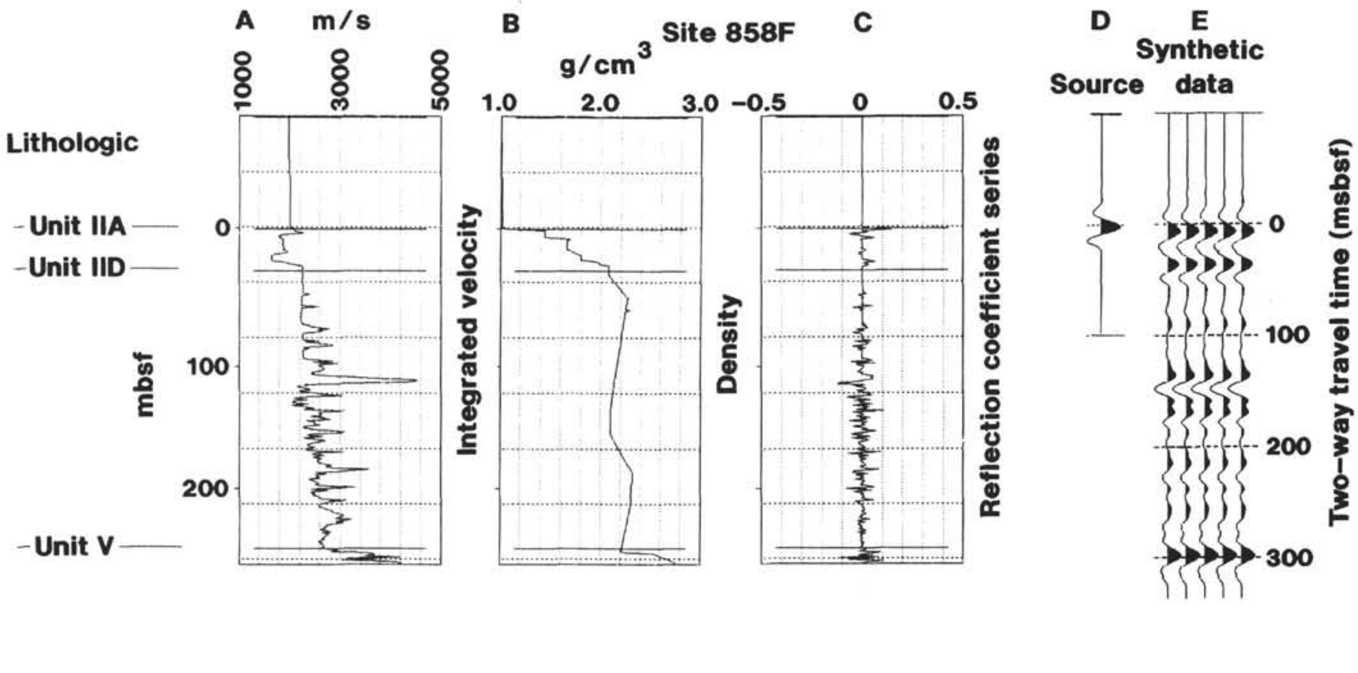

Figure 10. Calculation of synthetic seismograms. **A.** Velocity log. **B.** Density log. **C.** Reflectivity sequence. **D.** Source function. **E.** Synthetic traces. Source was taken from seafloor reflection of multichannel data.

bidites. Sediments in both holes have been altered relative to normal deep-water sediments, but a significantly higher degree of alteration has occurred under the active vent.

ACKNOWLEDGMENTS

We thank R. Franklin for assistance in drafting figures and E.E. Davis, A.T. Fisher, J. Miller, and J. Morton for their reviews.

REFERENCES*

Davis, E.E., Mottl, M.J., Fisher, A.T., et al., 1992. *Proc. ODP, Init. Repts.,* 139: College Station, TX (Ocean Drilling Program).

* Abbreviations for names of organizations and publications in ODP reference lists follow the style given in *Chemical Abstracts Service Source Index* (published by American Chemical Society).

Davis, E.E., and Villinger, H., 1992. Tectonic and thermal structure of the Middle Valley sedimented rift, northern Juan de Fuca Ridge. *In* Davis, E.E., Mottl, M.J., Fisher, A.T., et al., *Proc. ODP, Init. Repts.,* 139: College Station, TX (Ocean Drilling Program), 9–41.

Dix, C.H., 1955. Seismic velocities from surface measurements. *Geophysics,* 20:68–86.

Goodfellow, W.G., Franklin, J.M., et al., in press. Sedimentology, mineralogy and geochemistry of massive sulphide and hydrothermally altered sediment in shallow cores, Middle Valley, Northern Juan de Fuca Ridge. *Bull.—Geol. Surv. Can.*

Hamilton, E.L., 1976. Variations of density and porosity with depth in deep-sea sediments. *J. Sediment. Petrol.,* 46:280–300.

————, 1980. Geoacoustic modeling of the seafloor. *J. Acoust. Soc. Am.,* 68:1313–1340.

Hyndman, R.D., and Drury, M.J., 1976. The physical properties of oceanic basement rocks from deep drilling on the Mid-Atlantic Ridge. *J. Geophys. Res.,* 81:4042–4052.

Johnson, G.R., and Olhoeft, G.R., 1984. Density of rocks and minerals. *In* Carmichael, R.S. (Ed.), *CRC Handbook of Physical Properties of Rocks* (Vol. 3): Boca Raton, FL (CRC Press), 1–38.

Rohr, K.M.M., Davis, E.E., and Hyndman, R.D., 1992. Multi-channel seismic reflection profiles across Middle Valley, northern Juan de Fuca Ridge. *Open-File Rep.—Geol. Surv. Can.,* 2476.

Sheriff, R.E., 1977. Limitations on resolution of seismic reflections and geologic detail derivable from them. *In* Payton, C.E. (Ed.), *Seismic Stratigraphy: Applications to Hydrocarbon Exploration.* AAPG Mem., 26:3–14.

Shipboard Scientific Party, 1992a. Site 857. *In* Davis, E.E., Mottl, M.J., Fisher, A.T., et al., *Proc. ODP, Init. Repts.,* 139: College Station, TX (Ocean Drilling Program), 283–429.

————, 1992b. Site 858. *In* Davis, E.E., Mottl, M.J., Fisher, A.T., et al., *Proc. ODP, Init. Repts.,* 139: College Station, TX (Ocean Drilling Program), 431–569.

Shumway, G., 1958. Sound velocity vs. temperature in water-saturated sediments. *Geophysics,* 23:494–505.

Skinner, B.J., 1966. Thermal expansion. *In* Clark, S.P., Jr. (Ed.), 1966. *Handbook of Physical Constants.* Mem.—Geol. Soc. Am., 97.

Timur, A., 1977. Temperature dependence of compressional and shear wave velocities in rocks. *Geophysics,* 42:950–956.

Toksöz, M.N., Cheng, C.H., and Timur, A., 1976. Velocities of seismic waves in porous rocks. *Geophysics,* 41:621–645.

Date of initial receipt: 11 January 1993
Date of acceptance: 30 September 1993
Ms 139SR-257

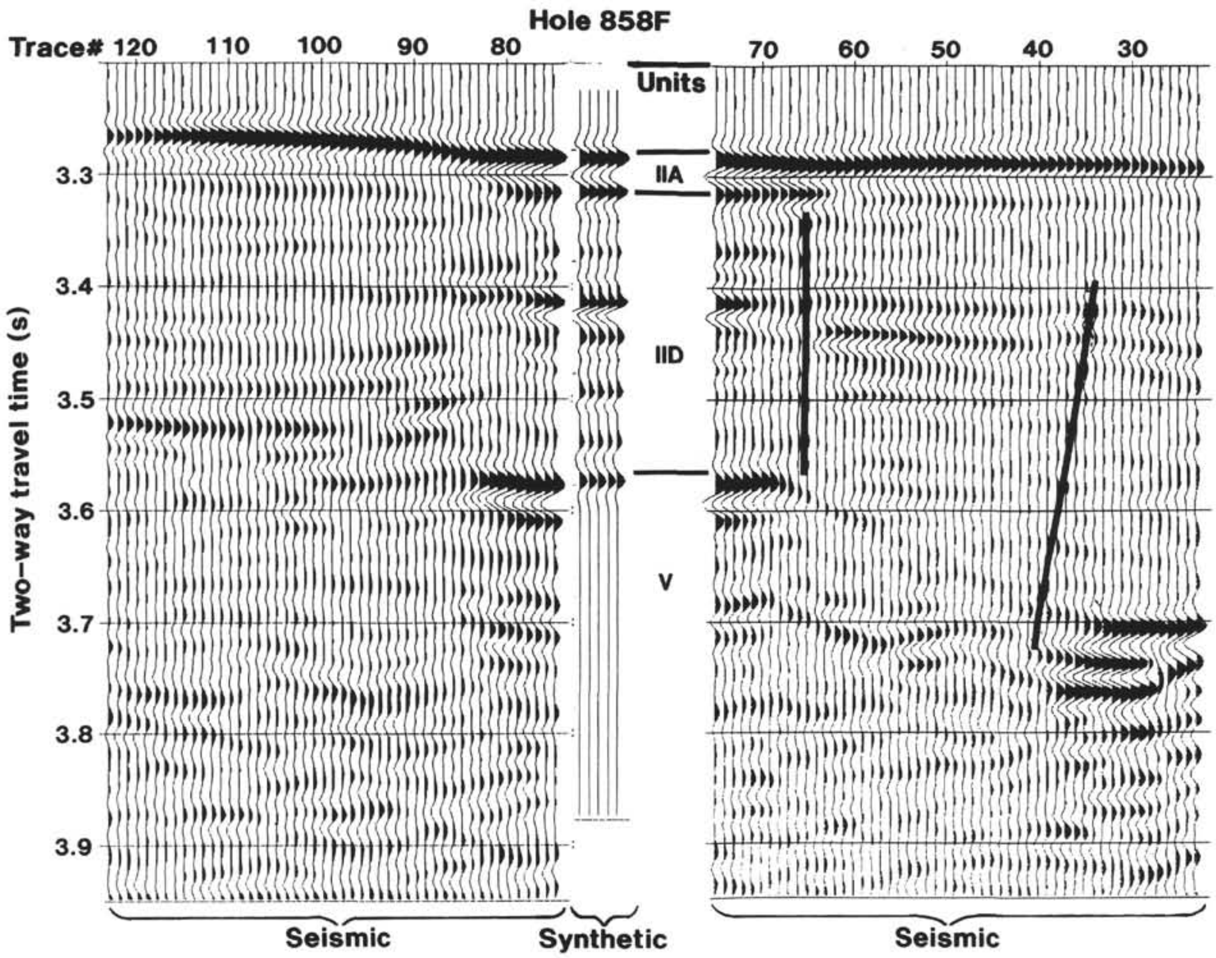

Figure 11. Synthetic seismograms for Hole 858F compared to near traces. The seafloor and basalt are the strongest reflectors; a reflection immediately beneath the seafloor can be modeled as the top of lithologic Subunit IID, highly altered sediments. A bright event in the sediments at 3.41 s is a high-velocity layer at 110 mbsf.

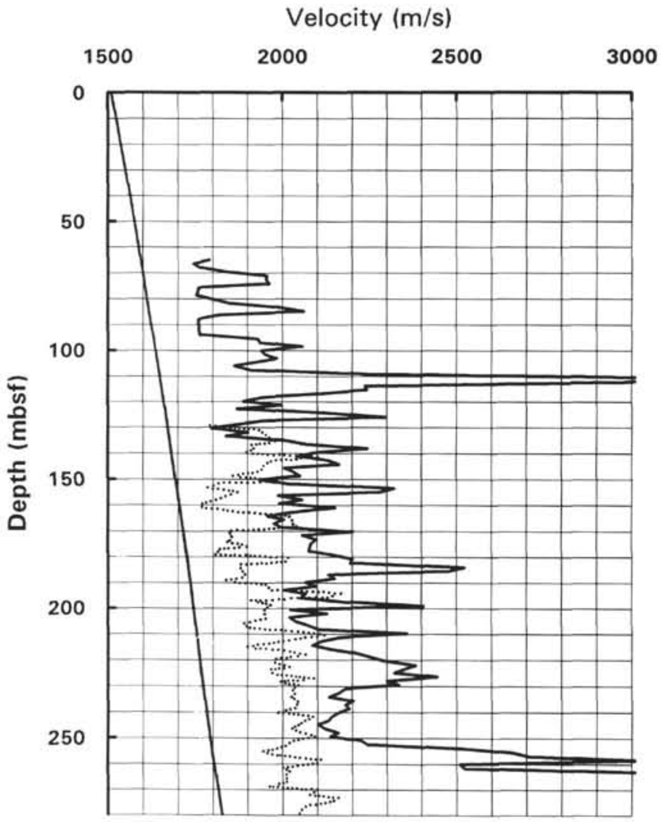

Figure 12. Velocity vs. depth profiles for Holes 857C (dotted line) and 858F (heavy line; as described in text) as well as velocity vs. depth expected for abyssal plain turbidites. Both holes have higher gradients between 130 and 250 mbsf than normal turbidites (thin solid line) (Hamilton, 1980).

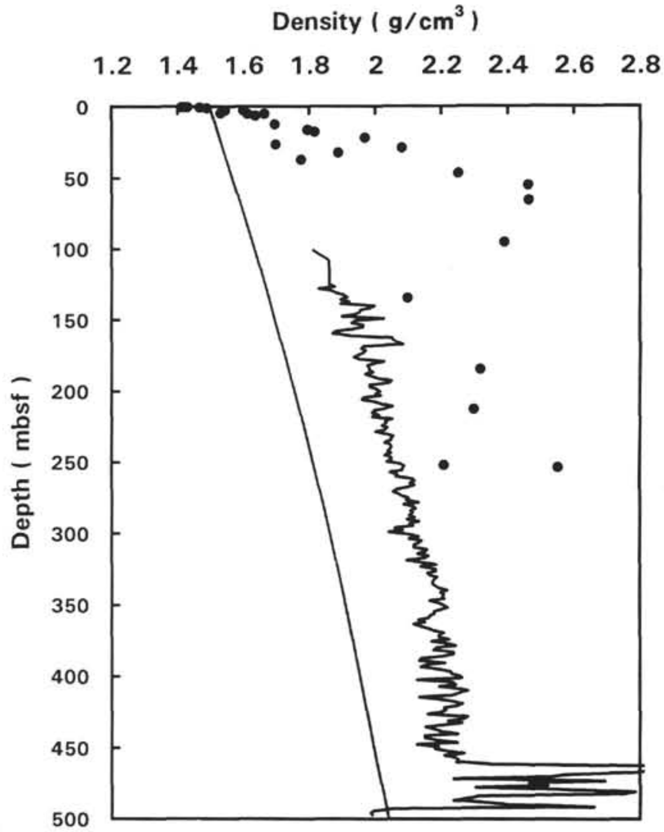

Figure 13. Density log for Hole 857C (heavy line) with lab measurements of density (dots) from Site 858 compared to density expected in normal turbidites (thin solid line) (Hamilton, 1976).

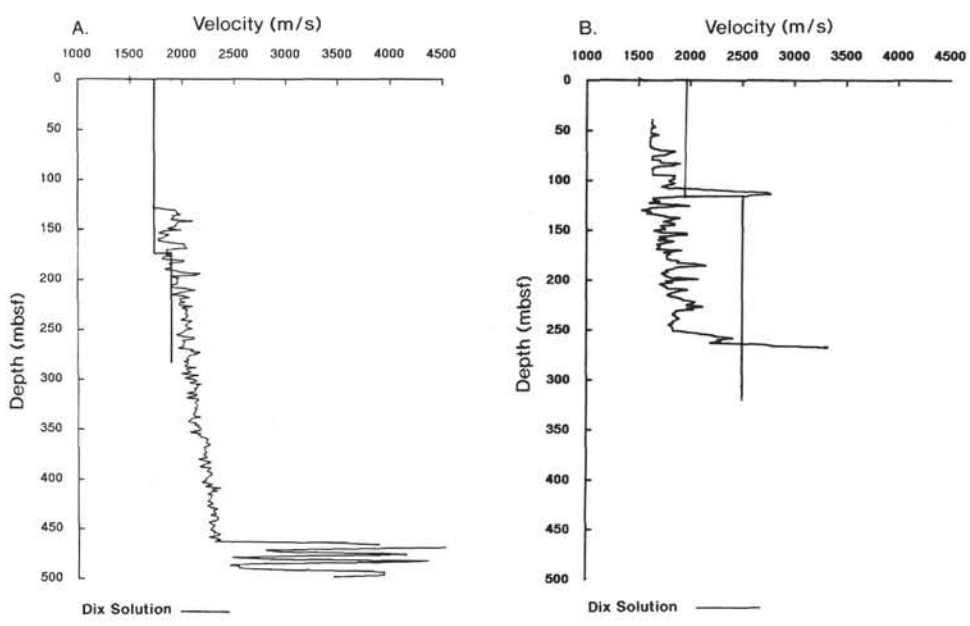

Figure 14. Comparison of velocities interpreted using Dix (1955) equations on wide-angle reflection data and velocities from sonic log. **A.** Hole 857C. **B.** Hole 858F.